

Title: How do biological traits affect brachiopod taxonomic
2 survival? A hierarchical Bayesian approach.

Running title: How do biological traits affect taxonomic survival?

4 **Author:** Peter D Smits, psmits@uchicago.edu, Committee on Evolutionary
Biology, University of Chicago

6 **Keywords:** extinction, macroevolution, macroecology, Paleozoic, selection

Word count: ?

8 **Table count:** 0.

Figure count: 9 main text, 3 supplement.

10 **Data archival location:** Dryad.

Abstract

While the effect of geographic range on extinction risk is well documented, the effects of other traits are less well known. Here, I analyze patterns of Paleozoic brachiopod genus durations and their relationship to geographic range, affinity for epicontinental seas versus open ocean environments, and body size. Additionally, I allow for environmental affinity to have a nonlinear effect on duration. Using a hierarchical Bayesian modeling approach, I also model the possible interaction between the effects of the biological traits and a taxon's time of origination. I find evidence that as extinction risk increases, the expected strength of the selection gradient on biological traits (except body size) increases. This manifests as greater expected differences in extinction risk for each unit change in geographic range and environmental preference during periods of high extinction risk, as opposed to a much flatter expected selection gradient during periods of low extinction risk. I find weak evidence for a nonlinear relationship between environmental preference and extinction risk such that "generalists" have a lower expected extinction risk than either "specialists". Importantly, I find that as extinction risk increases, the peakedness of this relationship is expected to increase as well. These results demonstrate the importance of directly modeling the structure inherent in the observed data as a means to better understand which processes may have been driving the observed patterns of diversification.

1 Introduction

How do biological traits affect extinction risk? Jablonski (1986) observed that during periods of high extinction risk, the effects of biological traits on survival decreased in size. However, this pattern was weakest/absent in the effect of geographic range on survival (Jablonski, 1986). Biological traits are defined here

38 as descriptors of a taxon’s adaptive zone, which is the set of biotic–biotic and
biotic–abiotic interactions that a taxon can experience (Simpson, 1944). In
40 effect, these are descriptors of a taxon’s broad-sense ecology.

Jablonski (1986) phrased their conclusions in terms of background versus mass
42 extinction, but this scenario is readily transferable to a continuous variation
framework as there is no obvious distinction in terms of extinction rate between
44 these two states (Wang, 2003). Additionally, the Jablonski (1986) scenario has
strong model structure requirements in order to test its proposed
46 macroevolutionary mechanism; not only do the taxon trait effects need to be
modeled, but the relationships between these effects need to be modeled as well.
48 There are two end-member macroevolutionary mechanisms which may underly
the pattern observed by Jablonski (1986) are: the effect of geographic range on
50 predictive survival remains constant and those of other biological traits decrease,
and the effect of geographic range in predicting survival increases and those of
52 other biological traits stay constant. Reality, of course, may fall somewhere
along the continuum between these two opposites.

54 I model taxon durations because trait based differences in extinction risk should
manifest as differences in taxon durations. Namely, a taxon with a beneficial
56 trait should survive longer, on average, than a taxon without that beneficial
trait. Conceptually, taxon survival can be considered an aspect of “taxon fitness”
58 along with expected lineage specific branching/origination rate (Cooper, 1984,
Palmer and Feldman, 2012). The analysis of taxon durations, or time from
60 origination to extinction, falls under the purview of survival analysis, a field of
applied statistics commonly used in health care (Klein and Moeschberger, 2003)
62 but has a long history in paleontology (Simpson, 1944, 1953, Van Valen, 1973,
1979).

64 Geographic range is widely considered the most important taxon trait for
estimating differences in extinction risk at nearly all times with large geographic
66 range associated with low extinction risk (Jablonski, 1986, 1987, Jablonski and
Roy, 2003, Payne and Finnegan, 2007). I expect this to hold true nearly always.
68 Miller and Foote (2009) demonstrated that during several mass extinctions taxa
associated with open-ocean environments tend to have a greater extinction risk
70 than those taxa associated with epicontinental seas. During periods of
background extinction, however, they found no consistent difference between
72 taxa favoring either environment. These two environment types represent the
primary environmental dichotomy observed in ancient marine systems (Miller
74 and Foote, 2009, Peters, 2008, Sheehan, 2001).

Epicontinental seas are a shallow-marine environment where the ocean has
76 spread over the surface of a continental shelf with a depth typically less than
100m. In contrast, open-ocean coastline environments have much greater
78 variance in depth, do not cover the continental shelf, and can persist during
periods of low sea level. Because of this, it is strongly expected that taxa which
80 favor epicontinental seas would be at great risk during periods of low sea levels,
such as during glacial periods, where these seas are drained. During the
82 Paleozoic, epicontinental seas were widely spread globally but declined over the
Mesozoic and eventually disappeared during the Cenozoic as open-ocean
84 coastlines became the dominant shallow-marine setting (Johnson, 1974, Miller
and Foote, 2009, Peters, 2008).

86 Given the above information, I predict that as extinction risk increases, taxa
associated with open-ocean environments should generally increase in extinction
88 risk versus those that favor epicontinental seas. Additionally, there is a possible
nonlinear relationship between environmental preference and taxon duration. A
90 long standing hypothesis is that generalists or unspecialized taxa will have

greater survival than specialists (Baumiller, 1993, Liow, 2004, 2007, Nürnberg
92 and Aberhan, 2013, 2015, Simpson, 1944). In this analysis I allowed for
environmental preference to possibly have a parabolic effect on taxon duration
94 Body size, measured as shell length (Payne et al., 2014), was also considered as
a potentially informative covariate. Body size is a proxy for metabolic activity
96 and other correlated life history traits (Payne et al., 2014). There is no strong
hypothesis of how body size effects extinction risk in brachiopods, meaning a
98 positive, negative, or zero effect are all plausible.

I adopt a hierarchical Bayesian survival modeling approach, which represents a
100 conceptual and statistical unification of the paleontological dynamic and cohort
survival analytic approaches (Baumiller, 1993, Foote, 1988, Raup, 1975, 1978,
102 Simpson, 2006, Van Valen, 1973, 1979). By using a Bayesian framework I am
able to quantify the uncertainty inherent in the estimates of the effects of
104 biological traits on survival, especially in cases where the covariates of interest
(i.e. biological traits) are themselves known with error.

106 **2 Materials and Methods**

2.1 Fossil occurrence information

108 The dataset analyzed here was sourced from the Paleobiology Database
(<http://www.paleodb.org>) which was then filtered based on taxonomic,
110 temporal, stratigraphic, and other occurrence information that was necessary
for this analysis. These filtering criteria are very similar to those from Foote and
112 Miller (2013) with an additional constraint of being present in the body size
data set from Payne et al. (2014). Epicontinental versus open-ocean assignments
114 for each fossil occurrence are partially based on those from Miller and Foote

(2009), with additional occurrences assigned similarly (Miller and Foote,
116 personal communication).

Sampled occurrences were restricted to those with paleolatitude and
118 paleolongitude coordinates, assignment to either epicontinental or open-ocean
environment, and belonging to a genus present in the body size dataset (Payne
120 et al., 2014). Genus duration was calculated as the number of geologic stages
from first appearance to last appearance, inclusive. Genera with a last
122 occurrence in or after Changhsingian stage were right censored at the
Changhsingian. Genera with a duration of only one stage were left censored
124 (Appendix C). The covariates used to model genus duration were geographic
range size (r), environmental preference (v, v^2), and body size (m).

126 Geographic range was calculated using an occupancy approach. First, all
occurrences were projected onto an equal-area cylindrical map projection. Each
128 occurrence was then assigned to one of the cells from a 70×34 regular raster
grid placed on the map. Each grid cell represents approximately 250,000 km².
130 The map projection and regular lattice were made using shape files from
<http://www.natureearthdata.com/> and the **raster** package for R (Hijmans,
132 2015).

For each stage, the total number of occupied grid cells, or cells in which a fossil
134 occurs, was calculated. Then, for each genus, the number of grid cells occupied
by that genus was calculated. Dividing the genus occupancy by the total
136 occupancy gives the relative occupancy of that genus. Mean relative genus
occupancy was then calculated as the mean of the per stage relative occupancies
138 of that genus.

Body size data was sourced directly from Payne et al. (2014). Because those
140 measurements are presented without error, a measurement error model similar

to the one for environmental affinity could not be implemented (Appendix A).

142 Prior to analysis, geographic range and body size were transformed and
standardized in order to improve interpretability of the results. Geographic
144 range, which can only vary between 0 and 1, was logit transformed. Body size,
which is defined for all positive real values, was natural log transformed. These
146 covariates were then standardized by mean centering and dividing by two times
their standard deviation following Gelman and Hill (2007).

148 **2.2 Analytical approach**

Hierarchical modelling, sometimes called “mixed-effects modeling,” is a
150 statistical approach which explicitly takes into account the structure of the
observed data in order to model both the within and between group variance
152 (Gelman et al., 2013, Gelman and Hill, 2007). The units of study (e.g. genera)
each belong to a single grouping (e.g. origination cohort). These groups are
154 considered draws from a shared probability distribution (e.g. all cohorts,
observed and unobserved). The group-level parameters are then estimated
156 simultaneously as the other parameters of interest (e.g. covariate effects)
(Gelman et al., 2013). The subsequent estimates are partially pooled together,
158 where parameters from groups with large samples or effects remain large while
those of groups with small samples or effects are pulled towards the overall
160 group mean.

This partial pooling is one of the greatest advantages of hierarchical modeling.
162 By letting the groups “support” each other, parameter estimates then better
reflect our statistical uncertainty. Additionally, this partial pooling helps control
164 for multiple comparisons and possibly spurious results as effects with little
support are drawn towards the overall group mean (Gelman et al., 2013,

166 Gelman and Hill, 2007).

All covariate effects (regression coefficients), as well as the intercept term
168 (baseline extinction risk), were allowed to vary by group (origination cohort).
The covariance/correlation between covariate effects was also modeled. This
170 hierarchical structure allows inference for how covariates effects may change
with respect to each other while simultaneously estimating the effects
172 themselves, propagating our uncertainty through all estimates.

Additionally, instead of relying on point estimates of environmental affinity, I
174 treat environmental affinity as a continuous measure of the difference between
the taxon’s environmental occurrence pattern and the background occurrence
176 pattern (Appendix A).

2.3 Survival model

178 Genus durations were modeled as time-till-event data (Klein and Moeschberger,
2003), with covariate information used in estimates of extinction risk as a
180 hierarchical regression model. Genus durations were assumed to follow either an
exponential or Weibull distribution. The use of either of these distributions
182 makes assumptions about how duration may effect extinction risk (Klein and
Moeschberger, 2003). The exponential distribution assumes that extinction risk
184 is independent of duration. In contrast, the Weibull distribution allows for age
dependent extinction via the shape parameter α , though only as a monotonic
186 function of duration. Importantly, the Weibull distribution is equivalent to the
exponential distribution when $\alpha = 1$.

188 The following variables are defined: y_i is the duration of genus i in geologic
stages, X is the matrix of covariates including a constant term, B_j is the vector
190 of regression coefficients for origination cohort j , Σ is the covariance matrix of

the regression coefficients, τ is the vector of scales the standard deviations of
 192 the between-cohort variation in regression coefficient estimates, and Ω is the
 correlation matrix of the regression coefficients.

194 The exponential model is defined

$$\begin{aligned}
 y_i &\sim \text{Exponential}(\lambda) \\
 \lambda_i &= \exp(\mathbf{X}_i B_{j[i]}) \\
 B &\sim \text{MVN}(\vec{\mu}, \Sigma) \\
 \Sigma &= \text{Diag}(\vec{\tau})\Omega\text{Diag}(\vec{\tau}) \\
 \mu_k &\sim \begin{cases} \mathcal{N}(0, \psi_k \nu) & \text{if } k \neq r, \text{ or} \\ \mathcal{N}(-1, 1) & \text{if } k = r \end{cases} \quad (1) \\
 \tau_k &\sim \text{C}^+(1) \\
 \psi_k &\sim \text{C}^+(1) \text{ if } k \neq r \\
 \nu &\sim \text{C}^+(1) \\
 \Omega &\sim \text{LKJ}(2).
 \end{aligned}$$

Similarly, the Weibull model is defined

$$\begin{aligned}
y_i &\sim \text{Weibull}(\alpha, \sigma) \\
\sigma_i &= \exp\left(\frac{-(\mathbf{X}_i B_{j[i]})}{\alpha}\right) \\
B &\sim \text{MVN}(\vec{\mu}, \Sigma) \\
\Sigma &= \text{Diag}(\vec{\tau})\Omega\text{Diag}(\vec{\tau}) \\
\alpha &\sim \text{C}^+(2) \\
\mu_k &\sim \begin{cases} \mathcal{N}(0, \psi_k \nu) & \text{if } k \neq r, \text{ or} \\ \mathcal{N}(-1, 1) & \text{if } k = r \end{cases} \quad (2) \\
\tau_k &\sim \text{C}^+(1) \\
\psi_k &\sim \text{C}^+(1) \text{ if } k \neq r \\
\nu &\sim \text{C}^+(1) \\
\Omega &\sim \text{LKJ}(2).
\end{aligned}$$

196 The principle difference between this model and the previous (Eq. 1) is the
inclusion of the shape parameter α . Note that σ is approximately equivalent to
198 $1/\lambda$.

For an explanation of how this model was developed, parameter explanations,
200 and choice of priors, please see Appendix B. Note that these models (Eq. 1, 2)
do not include how the uncertainty in environmental affinity is included nor how
202 censored observations are included. For an explanation of both of these aspects,
see Appendices A and C.

2.4 Parameter estimation

The joint posterior was approximated using a Markov-chain Monte Carlo routine that is a variant of Hamiltonian Monte Carlo called the No-U-Turn Sampler (Hoffman and Gelman, 2014) as implemented in the probabilistic programming language Stan (Stan Development Team, 2014a). The posterior distribution was approximated from four parallel chains run for 10,000 draws each, split half warm-up and half sampling and thinned to every 10th sample for a total of 5000 posterior samples. Chain convergence was assessed via the scale reduction factor \hat{R} where values close to 1 ($\hat{R} < 1.1$) indicate approximate convergence. Convergence means that the chains are approximately stationary and the samples are well mixed (Gelman et al., 2013).

2.5 Model evaluation

Models were evaluated using both posterior predictive checks and an estimate of out-of-sample predictive accuracy. The motivation behind posterior predictive checks as tools for determining model adequacy is that replicated data sets using the fitted model should be similar to the original data (Gelman et al., 2013). Systematic differences between the simulations and observations indicate weaknesses of the model fit. An example of a technique that is very similar would be inspecting the residuals from a linear regression.

The strategy behind posterior predictive checks is to draw simulated values from the joint posterior predictive distribution, $p(y^{rep}|y)$, and then compare those draws to the empirically observed values (Gelman et al., 2013). To accomplish this, for each replicate, a single value is drawn from the marginal posterior distributions of each regression coefficient from the final model as well as α for the Weibull model (Eq. 1, 2). Then, given the covariate information \mathbf{X} ,

a new set of n genus durations are generated giving a single replicated data set
 230 y^{rep} . This is repeated 1000 times in order to provide a distribution of possible
 values that could have been observed given the model.

232 In order to compare the fitted model to the observed data, various graphical
 comparisons or test quantities need to be defined. The principal comparison
 234 used here is a comparison between non-parameteric approximation of the
 survival function $S(t)$ as estimated from both the observed data and each of the
 236 replicated data sets. The purpose of this comparison is to determine if the
 model approximates the same survival/extinction pattern as the original data.

238 The exponential and Weibull models were compared for out-of-sample predictive
 accuracy using the widely-applicable information criterion (WAIC) (Watanabe,
 240 2010). Out-of-sample predictive accuracy is a measure of the expected fit of the
 model to new data. However, because the Weibull model reduces to the
 242 exponential model when $\alpha = 1$ my interest is not in choosing between these
 models. Instead, comparisons of WAIC values are useful for better
 244 understanding the effect of model complexity on out-of-sample predictive
 accuracy. The calculation of WAIC used here corresponds to the “WAIC 2”
 246 formulation recommended by Gelman et al. (2013). For an explanation of how
 WAIC is calculated, see Appendix D. Lower values of WAIC indicate greater
 248 expected out-of-sample predictive accuracy than higher values.

3 Results

250 As stated above, posterior approximations for both the exponential and Weibull
 models achieved approximate stationarity after 10,000 steps, as all parameter
 252 estimates have an $\hat{R} < 1.1$.

Comparisons of the survival functions estimated from 1000 posterior predictive
 254 data sets to the estimated survival function of the observed genera demonstrates
 that both the exponential and Weibull models approximately capture the
 256 observed pattern of extinction (Fig. 1). The major difference in fit between the
 two models is that the Weibull model has a slightly better fit for longer lived
 258 taxa than the exponential model.

Additionally, the Weibull model is expected to have slightly better out-of-sample
 260 predictive accuracy when compared to the exponential model (WAIC 4576
 versus 4604, respectively). 1). Because the difference in WAIC between these
 262 two models is large, while results from both the exponential and Weibull models
 will be presented, only those from the Weibull model will be discussed.

Estimates of the overall mean covariate effects μ can be considered
 264 time-invariant generalizations for brachiopod survival during the Paleozoic (Fig.
 266 2). Consistent with prior expectations, geographic range size has a negative
 effect on extinction risk, where genera with large ranges having greater
 268 durations than genera with small ranges.

I find that while the mean estimate of the effect of body size on extinction risk
 270 is negative, implying that increasing body size decreases extinction risk, this
 estimate is within 2 standard deviations of 0 (mean $\mu_m = -0.09$, standard
 272 deviation 0.09; Fig. 2). Because of this, I infer that body size has no
 distinguishable effect on brachiopod taxonomic survival.

Interpretation of the effect of environmental preference v on duration is slightly
 274 more involved. Because a quadratic term is the equivalent of an interaction
 276 term, both μ_v and μ_{v^2} have to be interpreted together because it is illogical to
 change values of v without also changing values v^2 . To determine the nature of
 278 the effect of v on duration I calculated the multiplicative effect of environmental

preference on extinction risk.

280 Given mean estimated extinction risk $\tilde{\sigma}$, we can define the extinction risk multiplier of an observation with environmental preference v_i as

$$\frac{\tilde{\sigma}_i}{\tilde{\sigma}} = f(v_i) = \exp\left(\frac{-(\mu_v v_i + \mu_{v^2} v_i^2)}{\alpha}\right). \quad (3)$$

282 This function $f(v_i)$ has a y-intercept of $\exp(0)$ or 1 because it does not have a non-zero intercept term. Equation 3 can be either concave up or down. A
 284 concave down $f(v_i)$ may indicate that genera of intermediate environmental preference have greater durations than either extreme, and *vice versa* for
 286 concave up function.

The expected effect of environmental preference as a multiplier of expected
 288 extinction risk can then be visualized (Fig. 3). This figure depicts 1000 posterior predictive estimates of Eq. 3 across all possible values of v . The number
 290 indicates the posterior probability that the function is concave down, with generalists having lower extinction risk/greater duration than either type of
 292 specialist. Note that the inflection point/optimum of Fig. 3 is approximately $x = 0$, something that is expected given the estimate of μ_v (Fig. 2).

294 The matrix Σ describing the covariance between the different coefficients describes how these coefficients might vary together across the origination
 296 cohorts. Similar to how this was modeled (Eq. 1, 2), for interpretation purposes Σ can be decomposed into a vector of standard deviations $\vec{\tau}$ and a correlation
 298 matrix Ω .

The estimates of the standard deviation of between-cohort coefficient estimates
 300 τ indicate that some effects can vary greatly between-cohorts (Fig. 4). Coefficients with greater values of τ have greater between-cohort variation. The
 302 covariate effects with the greatest between origination cohort variation are β_r ,

β_v , and β_{v2} . Estimates of β_m have negligible between cohort variation, as there
 304 is less between cohort variation than the between cohort variation in baseline
 extinction risk β_0 . However the amount of between cohort variation in estimates
 306 of β_{v2} means that it is possible for the function describing the effect of
 environmental affinity to be upward facing for some cohorts (Eq. 3), which
 308 corresponds to environmental generalists being shorted lived than specialists in
 that cohort.

310 The correlation terms of Ω (Fig. 5) describe the relationship between the
 coefficients and how their estimates may vary together across cohorts. The
 312 correlations between the intercept term β_0 and the effects of the taxon traits are
 of particular interest for evaluating the Jablonski (1986) scenario (Fig. 5 first
 314 column/last row). Keep in mind that when β_0 is low, extinction risk is low; and
 conversely, when β_0 is high, then extinction risk is high.

316 Marginal posterior probabilities of the correlations between the level of baseline
 extinction risk β_0 and the effects of the taxon traits indicate that the correlation
 318 between expected extinction risk and both geographic range β_r and β_{v2} are of
 particular note (Fig. 6).

320 There is approximately a 98% probability that β_0 and β_r are negatively
 correlated (Fig. 6), meaning that as extinction risk increases, the
 322 effect/importance of geographic range on genus duration increases. This means
 that increases in baseline extinction rate are correlated with an increased
 324 importance of geographic range size. There is a 93% probability that β_0 and β_{v2}
 are negatively correlated (Fig. 6), meaning that as extinction risk increases, the
 326 peakedness of $f(v_i)$ increases and the relationship tends towards concave down.
 Additionally, there is a 97% probability that values of β_r and β_{v2} are positively
 328 correlated (Mean correlation 0.51, standard deviation 0.23).

While the overall group level estimates are of particular importance when
 330 defining time-invariant differences in extinction risk, it is also important and
 useful to analyze the individual level parameter estimates in order to better
 332 understand how parameters actually vary across cohorts.

In comparison to the overall mean extinction risk μ_0 , cohort level estimates β_0
 334 show some amount of variation through time as expected by estimates of τ_0
 (Fig. 7). A similar, if slightly greater, amount of variation is also observable in
 336 cohort estimates of the effect of geographic range β_r (Fig. 8). Again, smaller
 values of β_0 correspond to lower expected extinction risk. Similarly, smaller
 338 values of β_r correspond to greater decrease in extinction risk with increasing
 geographic range

How the effect of environmental affinity varies between cohorts can be observed
 340 by using the cohort specific coefficients estimates. Following the same procedure
 by using the cohort specific estimates of β_v and β_{v^2} for
 342 μ_v and μ_{v^2} , the cohort specific effect of environmental preference as a multiplier
 of mean extinction risk can be calculated. This was done only for the Weibull
 344 model, though the observed pattern should be similar for the exponential model.

As expected based on the estimates of τ_v and τ_{v^2} , there is greater variation in
 346 the peakedness of $f(v_i)$ than there is variation between concave up and down
 functions (Fig. 9). 12 of the 33 cohorts have less than 50% posterior probability
 348 that generalists are potentially expected to be shorter lived than specialists,
 though two of those cases have approximately a 50% probability of being either
 350 concave up or down. This is congruent with the 0.72 posterior probability that
 352 μ_{v^2} is positive/ $f(v_i)$ is concave down.

Additionally, for some cohorts there is a quite striking pattern where the effect
 354 of environmental preference v has a nearly-linear relationship (Fig. 9). These are

primarily scenarios where one of the end member preferences is expected to
 356 have a greater duration than either intermediate or the opposite end member
 preference. Whatever curvature is present in these nearly-linear cases is due to
 358 the definition of $f(v)$ as it is not defined for non-negative values of σ (Eq. 3). For
 all stages between the Emsian through the Viséan, inclusive, intermediate
 360 preferences are of intermediate extinction risk when compared with
 epicontinental specialists (lowest risk) or open-ocean specialists (highest risk).
 362 This time period represents most of the Devonian through the early
 Carboniferous.

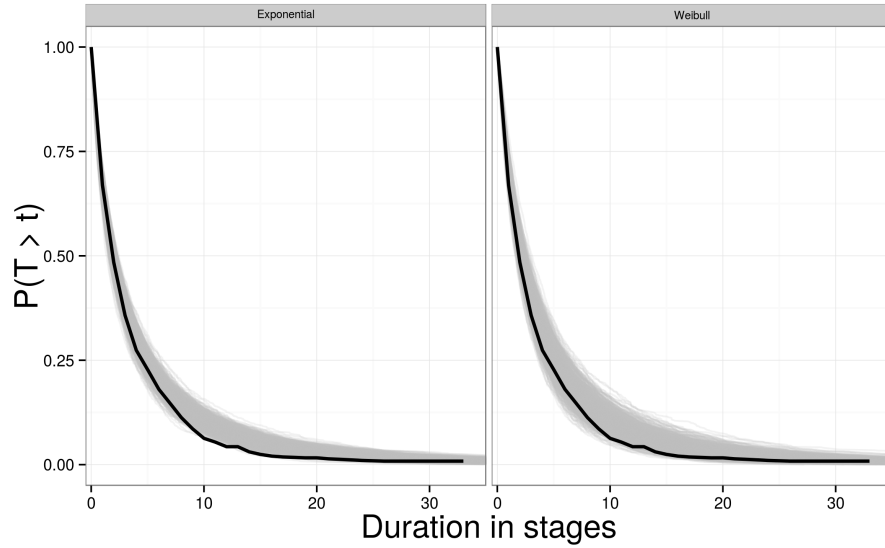


Figure 1: Comparison of empirical estimates of $S(t)$ versus estimates from 1000
 posterior predictive data sets. $S(t)$ corresponds to $P(T > t)$ as it is the probability
 that a given genus observed at age t will continue to live. This is equivalent to
 the probability that t is less than the genus' ultimate duration T . Note that the
 Weibull (left) model has noticeably better fit to the data than the exponential
 (right).

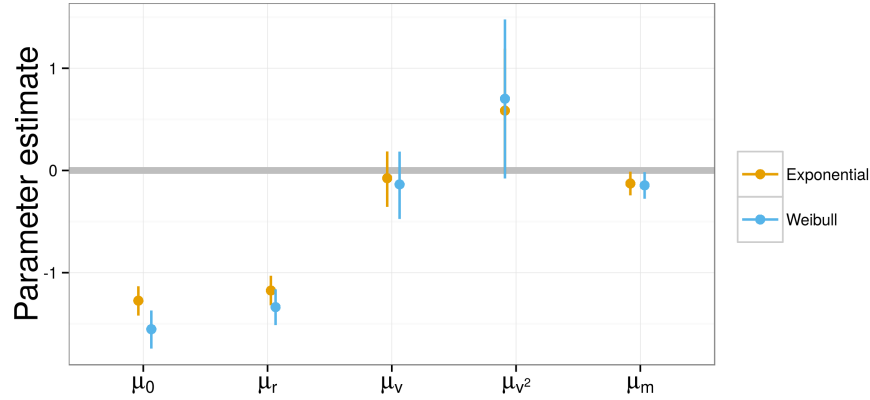


Figure 2: Estimates of the overall effects of the covariates on extinction risk. Included is also the estimate of μ_0 which corresponds to the intercept term or, because of standardization, the overall mean expected extinction risk. Estimates are presented for both the exponential (gold) and Weibull (blue) models. The point corresponds to the median of the posterior distribution, while the error bars correspond to the 80% credible intervals of the estimates.

364 4 Discussion

My results demonstrate that both the effects of geographic range and the
 366 peakedness/concavity of environmental preference are both negatively
 correlated with baseline extinction risk, meaning that as baseline extinction risk
 368 increases the effect sizes of both these traits are expected to increase (Fig. 6).
 This result supports neither of the two proposed macroevolutionary mechanisms
 370 for how biological traits should correlate with extinction risk. The observed
 correlation between the two effects as well as between the effects and baseline
 372 extinction risk instead implies that as baseline extinction risk increases, the
 strength of the total selection gradient on biological traits (except body size)
 374 increases. This manifests as greater differences in extinction risk for each unit
 difference in the biological covariates during periods of high extinction risk,
 376 while a relatively flatter selection gradient during periods of low extinction risk.

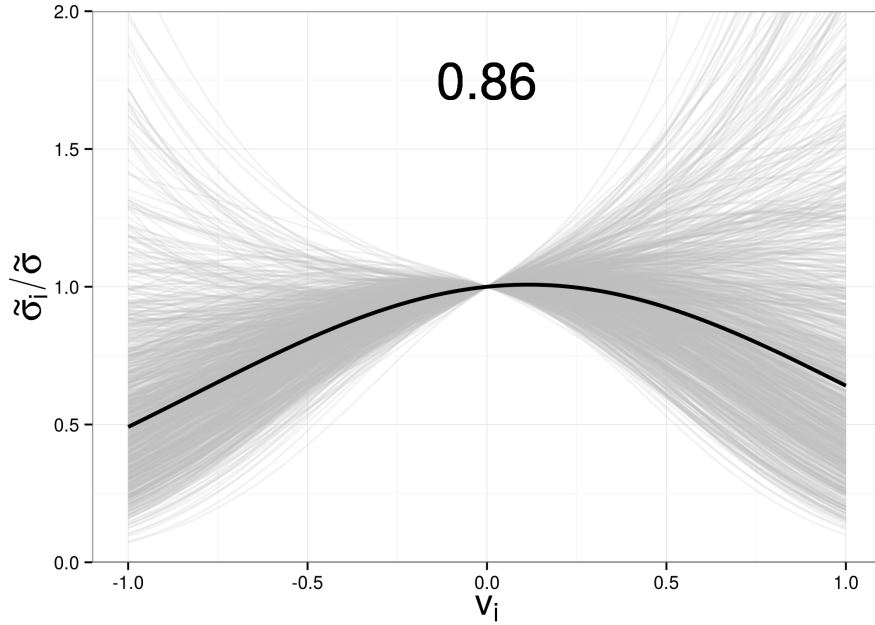


Figure 3: The overall expected relationship $f(v_i)$ between environmental affinity v_i and a multiplier of extinction risk (Eq. 3). Each grey line corresponds to a single draw from the posterior predictive distribution, while the black corresponds to the median of the posterior predictive distribution. The overall shape of $f(v_i)$ is concave down with an optimum of close 0, which corresponds to affinity approximately equal to the expectation based on background environmental occurrence rates.

There are two mass extinction events that are captured within the time frame
 378 considered here: the Ordovician-Silurian and the Frasnian-Famennian. The
 cohorts bracketing these events are worth considering in more detail.

380 The proposed mechanism for the end Ordovician mass extinction is a decrease
 in sea level and the draining of epicontinental seas due to protracted glaciation
 382 (Johnson, 1974, Sheehan, 2001). My results are broadly consistent with this
 scenario with both epicontinental and open-ocean specialists having a much
 384 lower expected duration than intermediate taxa (Fig. 9). All of the stages
 between the Darriwillian and the Llandovery, except the Hirnantian, have a

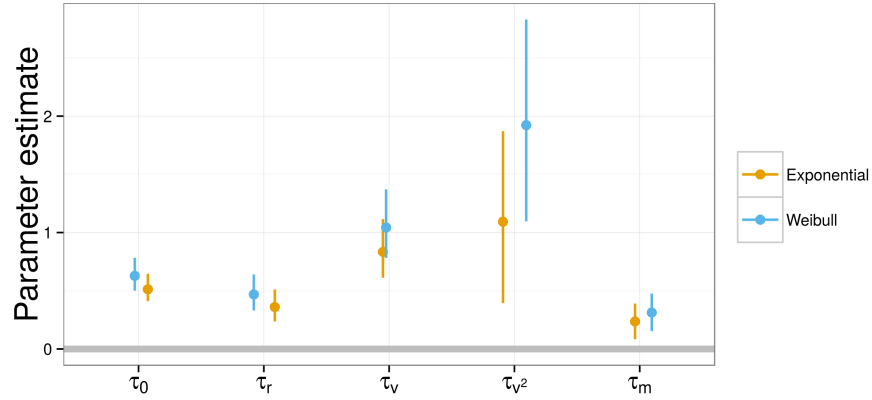


Figure 4: Estimates of the scale parameters describing the expected differences in the effect of the covariates, and of the intercept/baseline extinction risk, between cohorts. Higher values of τ correspond to greater expected differences between cohorts. Estimates are presented for both the exponential (gold) and Weibull (blue) models. The point corresponds to the median of the posterior distribution, while the error bars correspond to the 80% credible intervals of the estimates.

386 high probability (90+%) that $f(v)$ is concave down. The pattern for the
Darriwilian, which marks the supposed start of Ordovician glacial activity,
388 demonstrates that taxa tend to favor open-ocean environments are expected to
have a greater duration than either intermediate or epicontinental specialists, in
390 decreasing order.

For nearly the entire Devonian estimates of $f(v)$ indicate that one of the
392 environmental end members is favored over the other end member of
intermediate preference (Fig. 9). This is consistent with Miller and Foote (2009).
394 For almost the entirety the Givetian through the end of the Devonian and into
the Viséan, I find that epicontinental favoring taxa are expected to have a
396 greater duration than either intermediate or open-ocean specialists. Additionally,
for nearly the entire Devonian and through to the Viséan, the cohort-specific
398 estimates of $f(v)$ are concave-up. This is the opposite pattern than what is

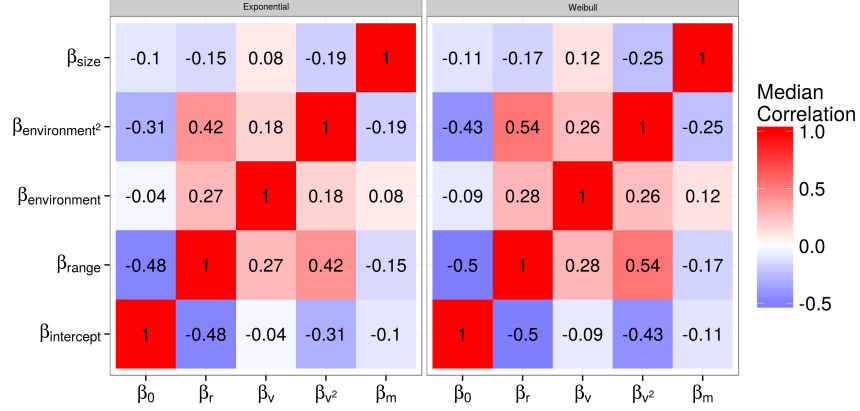


Figure 5: Heatmap for the median estimates of the terms of the correlation matrix Ω between cohort-level covariate effects. Both the exponential (left) and Weibull (right) models are presented. The off-diagonal terms are the correlation between the estimates of the cohort-level estimates of the effects of covariates, along with intercept/baseline extinction risk.

expected (Fig. 3). This result, however, seems to reflect the intensity of the
 400 seemingly nearly-linear difference in expected duration across the range of v) as
 opposed to an inversion of the weakly expected curvilinear pattern.

402 There is an approximate 72% posterior probability that taxa with intermediate
 environmental preferences are possibly expected to have a lesser extinction risk
 404 than either end members, the over all curvature of $f(v_i)$ is not very peaked,
 meaning that this relationship does not lead to very strong differences in
 406 extinction risk (Fig. 3). This result gives weak support for the hypothesis that,
 in general, environmental generalists survive for longer than environmental
 408 specialists (Liow, 2004, 2007, Nürnberg and Aberhan, 2013, 2015, Simpson,
 1944).

410 The variance in estimate of the overall $f(v_i)$ reflects the large between cohort
 variance in cohort specific estimates of $f(v_i)$ (Fig. 9). Given that there is only a
 412 72% posterior probability that the expected overall estimate of $f(v_i)$ is concave

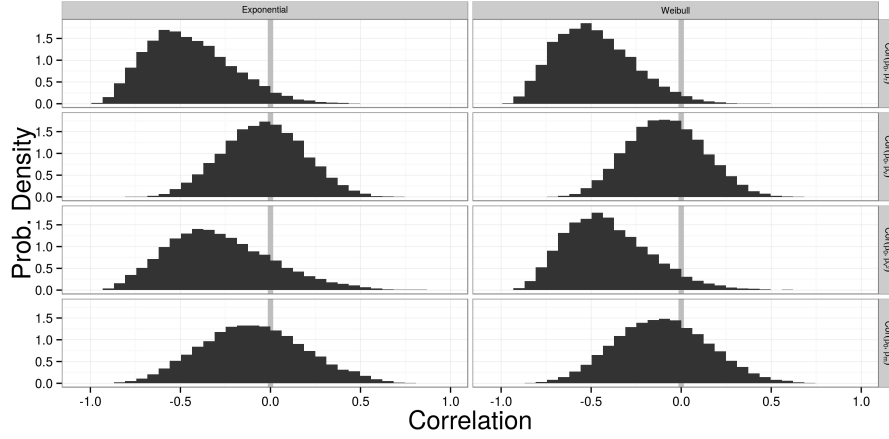


Figure 6: Marginal posterior distributions of the correlations between intercept terms/baseline extinction risk and the effects of each of the covariates. These are presented for both the exponential (left) and Weibull (right) models.

down, it is not surprising that there are some stages where the theorized

relationship is in fact reversed. Additionally, as discussed earlier, some of those
same stages where $f(v_i)$ does not resemble the theorized nonlinear relation with
the optimum in the middle, but are instead is highly skewed or effectively linear
(Fig. 9).

These results do not necessarily refute “survival of the unspecialized” as a
time-invariant generalization, but instead demonstrate how, while the expected
group-level estimate of $f(v_i)$ might favor one hypothesis, there is still enough
variability between cohorts so that in some realizations this pattern may not
hold or can even be reversed. These results are also consistent with aspects of
Miller and Foote (2009) who found that the effect of environmental preference
on extinction risk was quite variable and without obvious patterning during
times of background extinction.

This model can be improved through either increasing the number of analyzed
taxon traits, expanding the hierarchical structure of the model to include other

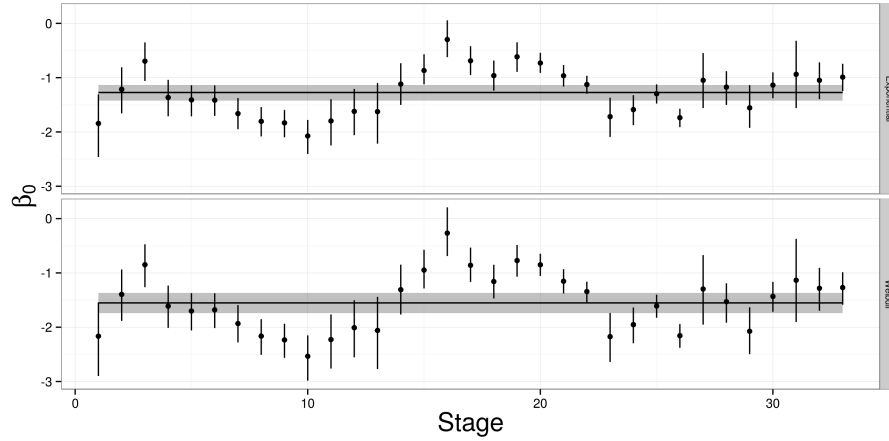


Figure 7: Comparison of cohort-specific estimates of β_0 presented along with the estimate for the overall baseline extinction risk. Points correspond to the median of the cohort-specific estimate, along with 80% credible intervals. The horizontal line is the median estimate of the overall baseline extinction risk along with 80% credible intervals. Results are presented for the exponential (top) and Weibull (bottom) models.

major taxonomic groups of interest, and the inclusion of explicit phylogenetic relationships between the taxa in the model as an additional hierarchical effect.

An example taxon trait that may be of particular interest is the affixing strategy or method of interaction with the substrate of the taxon. This trait has been found to be related to brachiopod survival (Alexander, 1977) so its inclusion may be of particular interest.

It is theoretically possible to expand this model to allow for comparisons within and between major taxonomic groups. This approach would better constrain the brachiopod estimates while also allowing for estimation of similarities and differences in cross-taxonomic patterns. The major issue surrounding this particular expansion involves finding an similarly well sampled taxonomic group that is present during the Paleozoic. Example groups include Crinoidea, Ostracoda, and other “Paleozoic” groups (Sepkoski Jr., 1981).

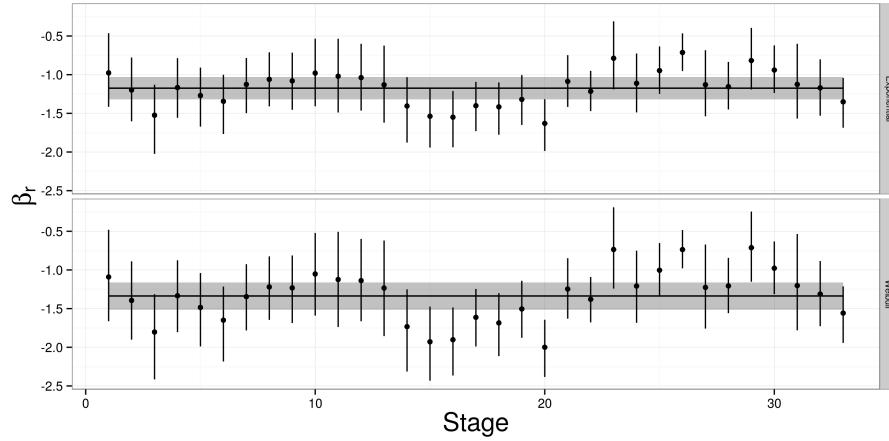


Figure 8: Comparison of cohort-specific estimates of the effect of geographic range on extinction risk β_r , presented along with the estimate for the overall effect of geographic range. Points correspond to the median of the cohort-specific estimate, along with 80% credible intervals. The horizontal line is the median estimate of the overall baseline extinction risk along with 80% credible intervals. Results are presented for the exponential (top) and Weibull (bottom) models.

Taxon traits like environmental preference or geographic range (Hunt et al.,
442 2005, Jablonski, 1987) are most likely heritable, at least phylogenetically
(Housworth et al., 2004, Lynch, 1991). Without phylogenetic context, this
444 analysis assumes that differences in extinction risk between taxa are
independent of those taxa's shared evolutionary history (Felsenstein, 1985). In
446 contrast, the origination cohorts only capture shared temporal context. The
inclusion of phylogenetic context as an additional individual level hierarchical
448 structure independent of origination cohort would allow for determining how
much of the observed variability is due to shared evolutionary history versus
450 actual differences associated with these taxonomic traits.

In summary, patterns of Paleozoic brachiopod survival were analyzed using a
452 fully Bayesian hierarchical survival modelling approach. Using a varying-slopes,
varying-intercepts approach I am able to model both the overall mean effect of

454 biological covariates on extinction risk while also modeling the correlation
 between origination cohort-specific estimates of covariate effects. I find that as
 456 baseline extinction risk increases, the strength of the selection gradient on
 biological traits (except body size) increases. This manifests as greater
 458 differences in extinction risk for each unit difference in the biological covariates
 during periods of high extinction risk, while a much flatter total selection
 460 gradient during periods of low extinction risk. I also find some support for
 “survival of the unspecialized” (Liow, 2004, 2007, Nürnberg and Aberhan, 2013,
 462 2015, Simpson, 1944) as a general characterization of the effect of environmental
 preference on extinction risk (Fig. 3), though there is heterogeneity between
 464 origination cohorts (Fig. 9). Generally, this study demonstrates the advantages
 of a hierarchical Bayesian framework for taking into account the structured
 466 nature of the data. Future studies of structured data should adopt similar
 strategies in order to best model our knowledge instead of ignoring that
 468 structure which can lead to poor and/or incorrect inference.

Acknowledgements

470 I would like to thank K. Angielczyk, M. Foote, P. D. Polly, and R. Ree for
 helpful discussion and advice. Additionally, thank you A. Miller for the
 472 epicontinental versus open-ocean assignments. This entire study would would
 not have been possible without the Herculean effort of the many contributors to
 474 the Paleobiology Database. In particular, I would like to thank J. Alroy, M.
 Aberhan, D. Bottjer, M. Clapham, F. Fürsich, N. Heim, A. Hendy, S. Holland,
 476 L. Ivany, W. Kiessling, B. Kröger, A. McGowan, T. Olszewski, P.
 Novack-Gottshall, M. Patzkowsky, M. Uhen, L. Villier, and P. Wager. This work
 478 was supported by a NASA Exobiology grant (NNX10AQ446) to M. Foote and

A. Miller. This is Paleobiology Database publication XXX.

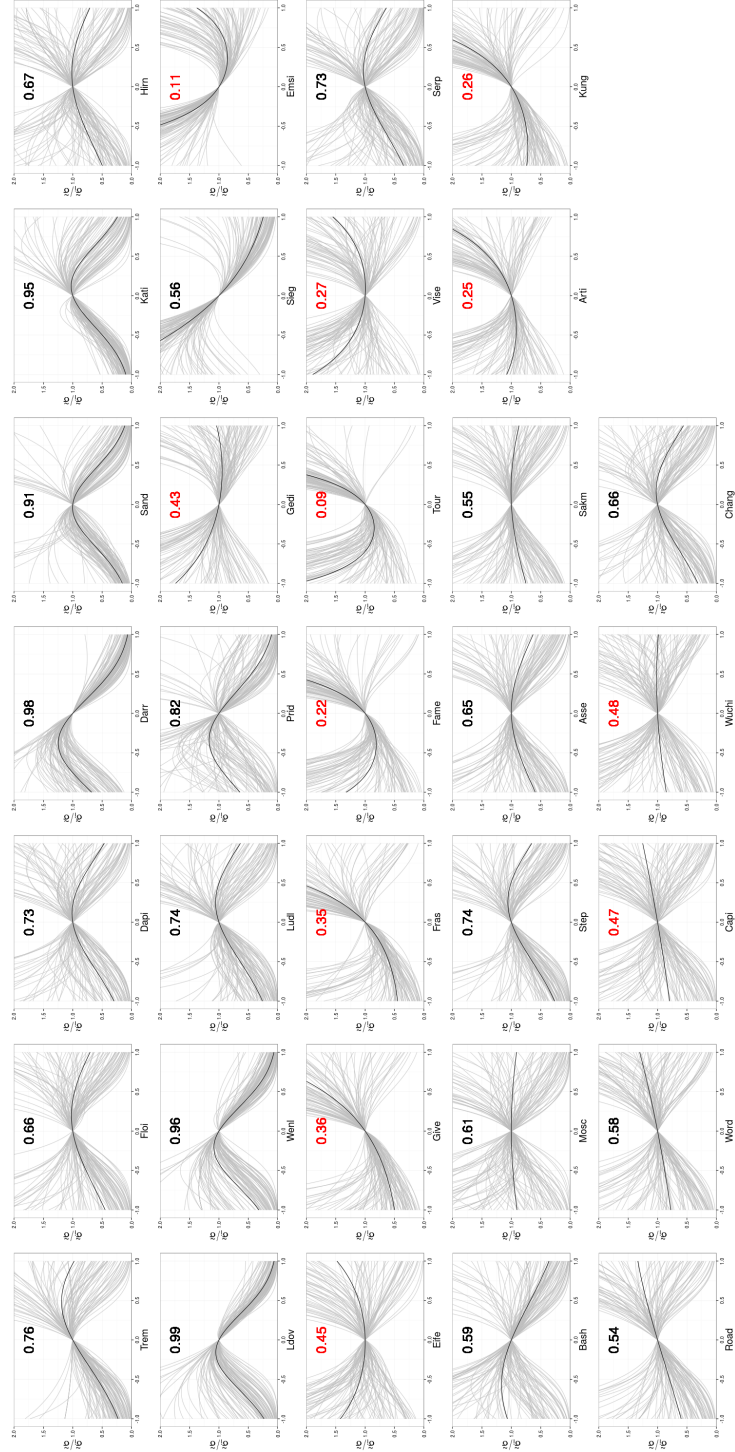


Figure 9: Comparison of the cohort-specific estimates of $f(v_i)$ (Eq. 3) for the 33 analyzed origination cohorts. The stage of origination is labeled on the x-axis of each panel. The oldest stage is in the upper left, while the youngest is in the lower left. The number in each panel corresponds to the posterior probability that $f(v_i)$ is concave down. Those that are highlighted in red have less than 51% posterior predictive probability that $f(v_i)$ is concave down.

References

- Alexander, R. R., 1977. Generic longevity of articulate brachiopods in relation to the mode of stabilization on the substrate. *Palaeogeography, Palaeoclimatology, Palaeoecology* 21:209–226.
- Baumiller, T. K., 1993. Survivorship analysis of Paleozoic Crinoidea: effect of filter morphology on evolutionary rates. *Paleobiology* 19:304–321.
- Carvalho, C. M., N. G. Polson, and J. G. Scott, 2009. Handling Sparsity via the Horseshoe. *in* Proceedings of the 12th International Conference on Artificial Intelligence and Statistics, vol. 5, Pp. 73–80.
- , 2010. The horseshoe estimator for sparse signals. *Biometrika* 97:465–480.
- Cooper, W. S., 1984. Expected time to extinction and the concept of fundamental fitness. *Journal of Theoretical Biology* 107:603–629.
- Felsenstein, J., 1985. Phylogenies and the comparative method. *American Naturalist* 125:1–15.
- Foote, M., 1988. Survivorship analysis of Cambrian and Ordovician Trilobites. *Paleobiology* 14:258–271.
- , 2006. Substrate affinity and diversity dynamics of Paleozoic marine animals. *Paleobiology* 32:345–366.
- Foote, M. and A. I. Miller, 2013. Determinants of early survival in marine animal genera. *Paleobiology* 39:171–192.
- Gelman, A., 2006. Prior distributions for variance parameters in hierarchical models. *Bayesian Analysis* 1:515–533.
- Gelman, A., J. B. Carlin, H. S. Stern, D. B. Dunson, A. Vehtari, and D. B.

504 Rubin, 2013. Bayesian data analysis. 3 ed. Chapman and Hall, Boca Raton,
FL.

506 Gelman, A. and J. Hill, 2007. Data Analysis using Regression and
Multilevel/Hierarchical Models. Cambridge University Press, New York, NY.

508 Hijmans, R. J., 2015. raster: Geographic data analysis and modeling. URL
<http://CRAN.R-project.org/package=raster>. R package version 2.3-24.

510 Hoffman, M. D. and A. Gelman, 2014. The No-U-Turn Sampler: Adaptively
Setting Path Lengths in Hamiltonian Monte Carlo. Journal of Machine
512 Learning Research 15:1351–1381.

Housworth, E. A., P. Martins, and M. Lynch, 2004. The Phylogenetic Mixed
514 Model. The American Naturalist 163:84–96.

Hunt, G., K. Roy, and D. Jablonski, 2005. Species-level heritability reaffirmed: a
516 comment on "On the heritability of geographic range sizes". American
Naturalist 166:129–135.

518 Ibrahim, J. G., M.-H. Chen, and D. Sinha, 2001. Bayesian Survival Analysis.
Springer, New York.

520 Jablonski, D., 1986. Background and mass extinctions: the alternation of
macroevolutionary regimes. Science 231:129–133.

522 ———, 1987. Heritability at the species level: analysis of geographic ranges of
cretaceous mollusks. Science 238:360–363.

524 Jablonski, D. and K. Roy, 2003. Geographical range and speciation in fossil and
living molluscs. Proceedings. Biological sciences / The Royal Society
526 270:401–6.

Johnson, J. G., 1974. Extinction of Perched Faunas. Geology 2:479–482.

- 528 Kiessling, W. and M. Aberhan, 2007. Environmental determinants of marine
benthic biodiversity dynamics through Triassic–Jurassic time. *Paleobiology*
530 33:414–434.
- Klein, J. P. and M. L. Moeschberger, 2003. *Survival Analysis: Techniques for*
532 *Censored and Truncated Data*. 2nd ed. Springer, New York.
- Liow, L. H., 2004. A test of Simpson’s ”rule of the survival of the relatively
534 unspecialized” using fossil crinoids. *The American naturalist* 164:431–43.
- , 2007. Does versatility as measured by geographic range, bathymetric
536 range and morphological variability contribute to taxon longevity? *Global Ecology and Biogeography* 16:117–128.
- 538 Lynch, M., 1991. Methods for the analysis of comparative data in evolutionary biology. *Evolution* 45:1065–1080.
- 540 Miller, A. I. and S. R. Connolly, 2001. Substrate affinities of higher taxa and the Ordovician Radiation. *Paleobiology* 27:768–778.
- 542 Miller, A. I. and M. Foote, 2009. Epicontinental seas versus open-ocean settings: the kinetics of mass extinction and origination. *Science* 326:1106–9.
- 544 Nürnberg, S. and M. Aberhan, 2013. Habitat breadth and geographic range predict diversity dynamics in marine Mesozoic bivalves. *Paleobiology*
546 39:360–372.
- , 2015. Interdependence of specialization and biodiversity in Phanerozoic
548 marine invertebrates. *Nature communications* 6:6602.
- Palmer, M. E. and M. W. Feldman, 2012. Survivability is more fundamental
550 than evolvability. *PloS one* 7:e38025.
- Payne, J. L. and S. Finnegan, 2007. The effect of geographic range on

552 extinction risk during background and mass extinction. *Proceedings of the*
National Academy of Sciences 104:10506–11.

554 Payne, J. L., N. A. Heim, M. L. Knope, and C. R. McClain, 2014. Metabolic
dominance of bivalves predates brachiopod diversity decline by more than 150
556 million years. *Proceedings of the Royal Society B* 281:20133122.

Peters, S. E., 2008. Environmental determinants of extinction selectivity in the
558 fossil record. *Nature* 454:626–9.

Raup, D. M., 1975. Taxonomic survivorship curves and Van Valen’s Law.
560 *Paleobiology* 1:82–96.

———, 1978. Cohort Analysis of generic survivorship. *Paleobiology* 4:1–15.

562 Sepkoski Jr., J. J., 1981. A factor analytic description of the Phanerozoic
marine fossil record. *Paleobiology* 7:36–53.

564 Sheehan, P., 2001. The late Ordovician mass extinction. *Annual Review of*
Earth and Planetary Sciences 29:331–364.

566 Simpson, C., 2006. Levels of selection and large-scale morphological trends.
Ph.D. thesis, University of Chicago.

568 Simpson, C. and P. G. Harnik, 2009. Assessing the role of abundance in marine
bivalve extinction over the post-Paleozoic. *Paleobiology* 35:631–647.

570 Simpson, G. G., 1944. *Tempo and Mode in Evolution*. Columbia University
Press, New York.

572 ———, 1953. *The Major Features of Evolution*. Columbia University Press,
New York.

574 Stan Development Team, 2014a. Stan: A c++ library for probability and
sampling, version 2.5.0. URL <http://mc-stan.org/>.

- 576 ———, 2014b. Stan Modeling Language Users Guide and Reference Manual,
Version 2.5.0. URL <http://mc-stan.org/>.
- 578 Van Valen, L., 1973. A new evolutionary law. *Evolutionary Theory* 1:1–30.
- , 1979. Taxonomic survivorship curves. *Evolutionary Theory* 4:129–142.
- 580 Wang, S. C., 2003. On the continuity of background and mass extinction.
Paleobiology 29:455–467.
- 582 Watanabe, S., 2010. Asymptotic Equivalence of Bayes Cross Validation and
Widely Applicable Information Criterion in Singular Learning Theory.
584 *Journal of Machine Learning Research* 11:3571–3594.

A Uncertainty in environmental preference

586 The calculation and inclusion of environmental affinity in the survival model is a
statistical procedure that takes into account our uncertainty based on where
588 fossils tend to occur. Because we cannot directly observe if a fossil taxon had
occurrences restricted to only a single environment, instead we can only
590 estimate its affinity with uncertainty. One advantage of using a Bayesian
analytical approach is that both parameters and data are considered random
592 samples from some underlying distribution, which means that it is possible to
model the uncertainty in our covariates of interest (Gelman et al., 2013). My
594 approach is conceptually similar to Simpson and Harnik (2009) but instead of
obtaining a single point estimate, an entire posterior distribution is estimated.

596 The first step is to determine the probability θ at which genus i occurs in an
epicontinental settings based on its own pattern of occurrences. Define e_i as the
598 number of occurrences of genus i in an epicontinental sea and o_i as the number of
occurrences of genus i not in an epicontinental sea (e.g. open ocean). Because
600 the value of interest is the probability of occurring in an epicontinental
environment, given the observed fossil record, I assume that probability follows
602 a binomial distribution. We can then define our sampling statement as

$$e_i \sim \text{Binomial}(e_i + o_i, \theta_i). \quad (4)$$

I used a flat prior for θ_i defined as $\theta_i \sim \text{Beta}(1, 1)$. Because the beta
604 distribution is the conjugate prior for the binomial distribution, the posterior is
easy to compute in closed form. The posterior probability of θ is then

$$\theta_i \sim \text{Beta}(e_i + 1, o_i + 1) \quad (5)$$

606 It is extremely important, however, to take into account the overall
environmental occurrence probability of all other genera present at the same
608 time as genus i . This is incorporated as an additional probability Θ . Define E_i
as the total number of other fossil occurrences (except for genus i) in
610 epicontinental seas during stages where i occurs and O_i as the number of other
fossil occurrences not on epicontinental seas. We can then define the sampling
612 statement as

$$E_i \sim \text{Binomial}(E_i + O_i, \Theta_i). \quad (6)$$

Again, I used a flat prior of Θ_i defined as $\Theta_i \sim \text{Beta}(1, 1)$. The posterior of Θ is
614 then simply defined as

$$\Theta_i \sim \text{Beta}(E_i + 1, O_i + 1) \quad (7)$$

I then define the environmental affinity of genus i as $v_i = \theta_i - \Theta_i$. v_i is a value
616 that can range between -1 and 1, where negative values indicate that genus i
tends to occur more frequently in open ocean environments than background
618 while positive values indicate that genus i tends to occur in epicontinental
environments.

620 While this approach is noticeably more complicated than previous ones (Foote,
2006, Kiessling and Aberhan, 2007, Miller and Connolly, 2001, Simpson and
622 Harnik, 2009) there are some important benefits to both using a continuous
measure of affinity as well directly modeling our uncertainty. In order to show
624 some of these benefits, I performed a simulation analysis of how
modal/maximum *a posteriori* (MAP) estimates versus full posterior estimates.

626 In this simulation, I first defined the “background” epicontinental occurrence θ_b
as 0.50 with a small amount of noise. This was represented as a beta distribution

$$\Theta_b = \text{Beta}(\alpha = 2500, \beta = 2500). \quad (8)$$

628 This choice of parameters for the distribution reflects the average number of
background occurrences for either epicontinental or open ocean environments
630 per genus.

Using this background occurrence ratio, I randomly generated the occurrence
632 patterns of 1000 simulated taxa. This was done at multiple sample sizes (1, 2, 3,
4, 5, 10, 25, 50, 100) in order to demonstrate the effects of increasing sample
634 size on the confidence of environmental affinity. For each simulated taxon I
calculated the full posterior distribution while assuming a flat Beta prior
636 (Beta(1, 1)). Using the full posterior I calculated the MAP probability of
occurring in epicontinental environments. The environmental affinity was
638 calculated for each of the simulated taxa using both the full posterior and the
MAP estimate. In this toy example, environmental affinity can range between
640 -0.5 and 0.5.

As should be expected, as sample size increases the distribution of MAP
642 estimates converge on the true value (Fig. 10). For taxa with less than 10
occurrences, the MAP estimate is biased towards extreme values. Note that the
644 mode of the beta distribution is not defined for situations where there were 0
draws of one of the environmental conditions. Instead, the vertical line is based
646 entirely on the observed occurrences which are technically the modal estimates
because they are the most frequently occurring/highest density.

648 In contrast, we can compare the true occurrence probability distribution versus
the posterior estimate for a given sample (Fig. 11). When sample sizes are low,
650 posterior estimates are flat and represent a compromise between the likelihood
and the flat prior (Eq. 5). Because of this, estimates from small sizes are less

likely to be overly biased towards the extremes. This is further emphasized by inspection of the estimates of environmental affinity for the simulated taxa (Fig. 12). Posterior estimates from simulated taxa with small sample size have a much broader distribution that both allows for the extreme observation but still captures the “true” value (0).

By defining environmental preference as the difference in full posterior estimates of occurrence probability, it is possible to include taxa with low sample sizes that are normally discarded (Foote, 2006, Kiessling and Aberhan, 2007, Miller and Connolly, 2001, Simpson and Harnik, 2009). Additionally, 55+% of observed Paleozoic brachiopod genera have less than 10 occurrences which is the range of sample sizes where MAP (or ML) estimates would be potentially most biased. This is preferable to finding the difference between the MAP estimates (blue line; Fig. 12).

B Survival model

The simplest model of genus duration includes no covariate or structural information. Define y_i as the duration in stages of genus i , where $i = 1, \dots, n$ and n is the number of observed genera. These two models are then simply defined as

$$\begin{aligned} y_i &\sim \text{Exponential}(\lambda) \\ y_i &\sim \text{Weibull}(\alpha, \sigma). \end{aligned} \tag{9}$$

λ, α , and σ are all defined for all positive reals. Note that λ is a “rate” or inverse-scale while σ is a scale parameter, meaning that $\frac{1}{\lambda} = \sigma$.

These simple models can then be expanded to include covariate information as predictors by reparameterizing λ or σ as a regression (Klein and Moeschberger,

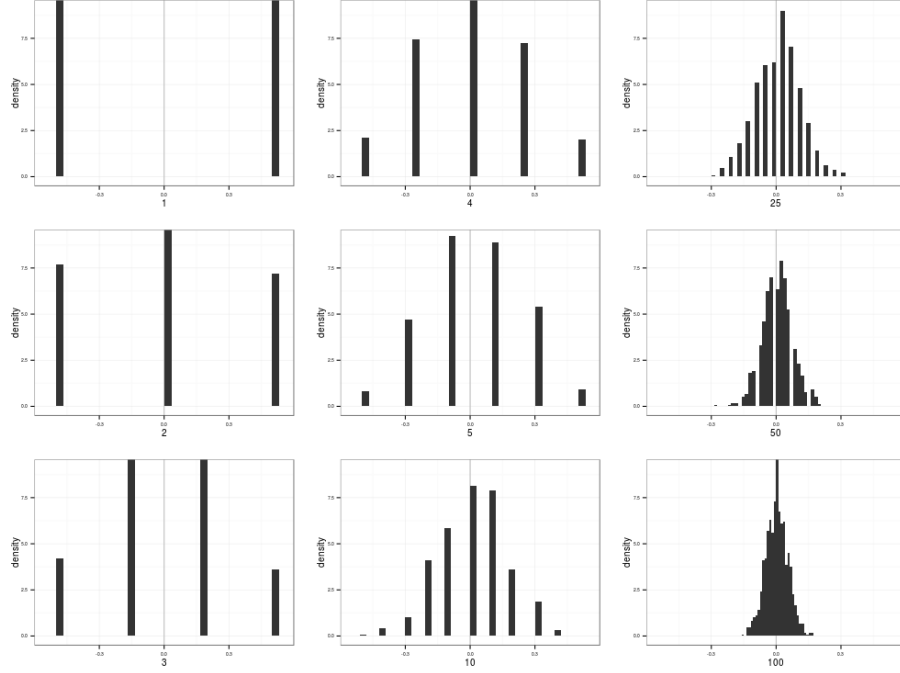


Figure 10: Histograms of the distributions of from the beta distribution defined in Eq. 8. As to be expected, as sample size increases the draws better resemble the underlying true distribution. Sample size is indicated as the label of the x-axis, increasing in column major order.

2003). Each of the covariates of interest is given its own regression coefficient (e.g. β_r) along with an intercept term β_0 . There are some additional complications to the parameterization of σ associated with the inclusion of α as well as for interpretability (Klein and Moeschberger, 2003). Both of these are then written as

$$\begin{aligned}\lambda_i &= \exp(\beta_0 + \beta_r r_i + \beta_v v_i + \beta_{v^2} v_i^2 + \beta_m m_i) \\ \sigma_i &= \exp\left(\frac{-(\beta_0 + \beta_r r_i + \beta_v v_i + \beta_{v^2} v_i^2 + \beta_m m_i)}{\alpha}\right).\end{aligned}\tag{10}$$

The quadratic term for environmental affinity v is to allow for the possible nonlinear relationship between environmental affinity and extinction risk.

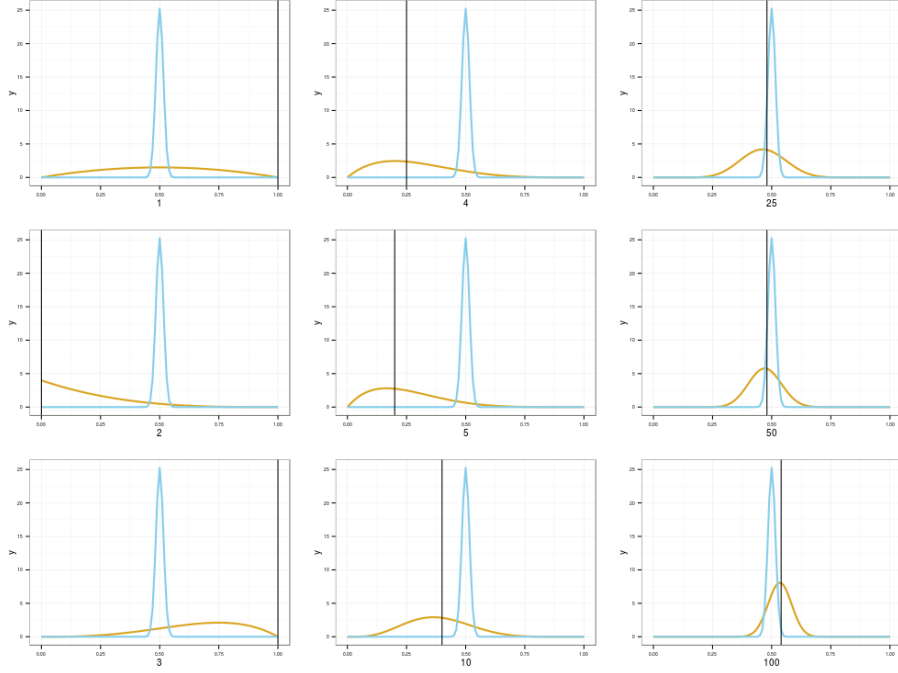


Figure 11: Comparisons of the underlying distribution (blue) to posterior estimates based on increasing sample size (gold). Each posterior estimate is represented for only a single realization of draws, each with sample size indicated as the x-axis label (increasing in column major order). Black vertical lines correspond to the MAP estimate of the simulated taxon’s affinity. This stands in contrast to the posterior distribution of expected affinity in gold.

The models which incorporate both equations 9 and 10 can then be further
682 expanded to allow all of the β coefficients, including β_0 , to vary with origination
cohort while also modeling their covariance and correlation. This is called a
684 varying-intercepts, varying-slopes model (Gelman and Hill, 2007). It is much
easier to represent and explain how this is parameterized using matrix notation.
686 First, define \mathbf{B} as $k \times J$ matrix of the k coefficients including the intercept term
($k = 5$) for each of the J cohorts. Second, define \mathbf{X} as a $n \times k$ matrix where each
688 column is one of the covariates of interest. Importantly, \mathbf{X} includes a columns of
all 1s which correspond to the constant term β_0 . Third, define $j[i]$ as the

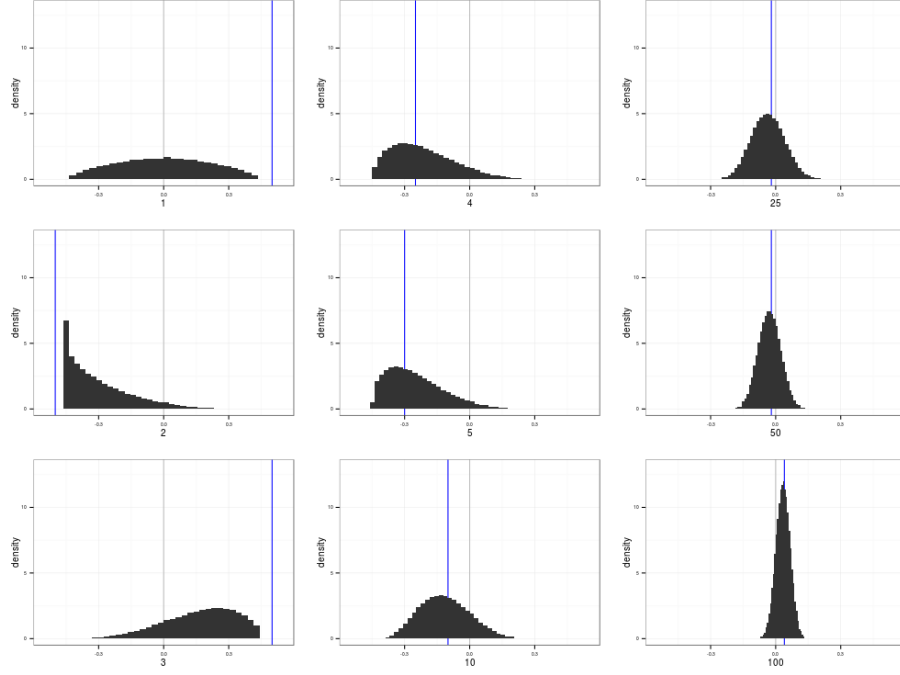


Figure 12: Histograms of the difference in the underlying occurrence distribution and the posterior distribution estimates from the previous graph (Fig. 11). The “true” value is included in all distributions of environmental affinities. Each affinity estimate is represented for only a single realization of draws, each with sample size indicated as the x-axis label (increasing in column major order). Blue vertical lines correspond to the difference in MAP estimates between the underlying distribution and the simulated taxon’s draws. This stands in contrast to the distribution of the differences between the simulated taxon and background.

690 origination cohort of genus i , where $j = 1, \dots, J$ and J is the total number of observed cohorts. We then rewrite λ and σ of equation 10 in matrix notation as

$$\begin{aligned}\lambda_i &= \exp(\mathbf{X}_i B_{j[i]}) \\ \sigma_i &= \exp\left(\frac{-(\mathbf{X}_i B_{j[i]})}{\alpha}\right).\end{aligned}\tag{11}$$

692 Because B is a matrix, I use a multivariate normal prior with unknown vector

of means μ and covariance matrix Σ . This is written as

$$B \sim \text{MVN}(\vec{\mu}, \Sigma) \quad (12)$$

where $\vec{\mu}$ is length k vector representing the overall mean of the distributions of β coefficients. Σ is a $k \times k$ covariance matrix of the β coefficients.

What remains is assigning priors the elements of $\vec{\mu}$ and the covariance matrix Σ . All elements of $\vec{\mu}$ except for μ_r were given horseshoe priors (Carvalho et al., 2009, 2010) while μ_r was given an informative normal prior ($\mu_r \sim \mathcal{N}(-1, 1)$).

Horseshoe priors are a strong regularizing priors with effectively infinite density at 0 and heavy, Cauchy-like tails (Carvalho et al., 2009, 2010) which allow weakly inferred effects to be strongly drawn towards 0 while truly strong effects can remain large. The horseshoe prior consists of a normal distribution with scale term that is the product between a global shrinkage parameter ν and a local shrinkage parameter ψ unique to each of the parameters of interest. These parameters are themselves given half-Cauchy priors (Eq. 1 and 2).

The prior for Σ is a bit more complicated due to its multivariate nature. Following the Stan Development Team (2014b), I modeled the scale terms separate from the correlation structure of the coefficients. This is possible because of the relationship between a covariance and a correlation matrix, defined as

$$\Sigma_B = \text{Diag}(\vec{\tau})\Omega\text{Diag}(\vec{\tau}) \quad (13)$$

where $\vec{\tau}$ is a length k vector of variances and $\text{Diag}(\tau)$ is a diagonal matrix.

I used a LKJ prior distribution for correlation matrix Ω as recommended by Stan Development Team (2014b). The LKJ distribution is a single parameter multivariate distribution where values of the parameter η greater than 1

concentrate density at the unit correlation matrix, which corresponds to no
716 correlation between the β coefficients. The scale parameters, $\vec{\tau}$, are given weakly
informative half-Cauchy (C^+) priors following Gelman (2006).

718 C Censored observations

A key aspect of survival analysis is the inclusion of censored, or incompletely
720 observed, data points (Ibrahim et al., 2001, Klein and Moeschberger, 2003). The
two classes of censored observations encountered in this study were right and
722 left censored observations. Right censored genera are those that did not go
extinct during the window of observation, or genera that are still extant. Left
724 censored observations are those taxa for which we know only an upper limit on
their duration.

726 In the context of this study, I considered all genera that had a duration of only
one geologic stage to be left censored as we do not have a finer degree of
728 resolution.

The key function for modeling censored observations is the survival function, or
730 $S(t)$. $S(t)$ corresponds to the probability that a genus having existed for t stages
will not have gone extinct while $h(t)$ corresponds to the instantaneous
732 extinction rate at taxon age t Klein and Moeschberger (2003). For an
exponential model, $S(t)$ is defined as

$$S(t) = \exp(-\lambda t), \quad (14)$$

734 and for the Weibull distribution $S(t)$ is defined as

$$S(t) = \exp\left(-\left(\frac{t}{\sigma}\right)^\alpha\right). \quad (15)$$

$S(t)$ is equivalent to the complementary cumulative distribution function,
 736 $1 - F(t)$ (Klein and Moeschberger, 2003).

For right censored observations, instead of calculating the likelihood as normal
 738 (Eq. 11) the likelihood of an observation is evaluated using $S(t)$. Conceptually,
 this approach calculates the likelihood of observing a taxon that existed for at
 740 least that long. For left censored data, instead the likelihood is calculated using
 $1 - S(t)$ which corresponds to the likelihood of observing a taxon that existed
 742 no longer than t .

The full likelihood statements incorporating fully observed, right censored, and
 744 left censored observations are then

$$\begin{aligned}\mathcal{L} &\propto \prod_{i \in C} \text{Exponential}(y_i | \lambda) \prod_{j \in R} S(y_j | \lambda) \prod_{k \in L} (1 - S(y_k | \lambda)) \\ \mathcal{L} &\propto \prod_{i \in C} \text{Weibull}(y_i | \alpha, \sigma) \prod_{j \in R} S(y_j | \alpha, \sigma) \prod_{k \in L} (1 - S(y_k | \alpha, \sigma))\end{aligned}\tag{16}$$

where C is the set of all fully observed taxa, R the set of all right censored taxa,
 746 and L the set of all left-censored taxa.

D Widely applicable information criterion

748 WAIC can be considered a fully Bayesian alternative to the Akaike information
 criterion, where WAIC acts as an approximation of leave-one-out
 750 cross-validation which acts as a measure of out-of-sample predictive accuracy
 (Gelman et al., 2013). WAIC is calculated starting with the log pointwise
 752 posterior predictive density calculated as

$$\text{lppd} = \sum_{i=1}^n \log \left(\frac{1}{S} \sum_{s=1}^S p(y_i | \theta^s) \right), \tag{17}$$

where n is sample size, S is the number posterior simulation draws, and Θ
754 represents all of the estimated parameters of the model. This is similar to
calculating the likelihood of each observation given the entire posterior. A
756 correction for the effective number of parameters is then added to lppd to
adjust for overfitting. The effective number of parameters is calculated,
758 following the recommendations of Gelman et al. (2013), as

$$p_{\text{WAIC}} = \sum_{i=1}^n V_{s=1}^S(\log p(y_i|\Theta^S)). \quad (18)$$

where V is the sample posterior variance of the log predictive density for each
760 data point.

Given both equations 17 and 18, WAIC is then calculated

$$\text{WAIC} = \text{lppd} - p_{\text{WAIC}}. \quad (19)$$

762 When comparing two or more models, lower WAIC values indicate better
out-of-sample predictive accuracy. Importantly, WAIC is just one way of
764 comparing models. When combined with posterior predictive checks it is
possible to get a more complete understanding of a model's fit to the data.